Insights into alternative prion protein topologies induced under high hydrostatic pressure

2004 J. Phys.: Condens. Matter 16 S1059

(http://iopscience.iop.org/0953-8984/16/14/016)

INSTITUTE OF PHYSICS PUBLISHING JOURNAL OF PHYSICS: CONDENSED MATTER

J. Phys.: Condens. Matter **16** (2004) S1059–S1065 PII: S0953-8984(04)74917-6

Insights into alternative prion protein topologies induced under high hydrostatic pressure

Joan Torrent[1], Maria Teresa Alvarez-Martinez[2], Frédéric Heitz[3], Jean-Pierre Liautard[2], Claude Balny[1] and Reinhard Lange[1]

[1] INSERM U128, IFR 122, 1919 Route de Mende, F-34293 Montpellier cedex 5, France
[2] INSERM U431, IFR 122, Place Eugène Bataillon, F-34095 Montpellier cedex 5, France
[3] CRBM, CNRS-UPR 1086, IFR 122, 1919 Route de Mende, F-34293 Montpellier cedex 5, France

Received 21 January 2004
Published 26 March 2004
Online at stacks.iop.org/JPhysCM/16/S1059
DOI: 10.1088/0953-8984/16/14/016

Abstract

The critical step in the pathogenesis of transmissible spongiform encephalopathies (TSEs) appears to be a conformational transition of a normal prion protein (PrP^{C}) into a misfolded isoform (PrP^{Sc}). To gain insight into the structural conversion of the prion protein we have exploited the use of high hydrostatic pressure combined with various spectroscopic techniques.

In vitro transitions of the recombinant PrP to a scrapie-like form have never resulted in an infectious structure. It is our hypothesis that the acquisition of the disease-causing conformation depends on folding pathways which are difficult to attain. We attempt to favour, via specific reaction conditions at high pressure, alternative routes of misfolding leading to a stable infectious amyloidogenic conformer. Our results have demonstrated the potential of high pressure to reveal various prion structural changes, which are inaccessible by conventional methods. Especially, we have characterized a pressure-induced conformer in which the normal α-helical structure is changed into a highly aggregated β-sheet conformation showing markedly increased resistance to proteolysis (key markers of potential infectious agents).

Our work may have important implications, not only for ultimately proving the protein-only hypothesis and for understanding the basic mechanism of the disease, but also for developing preventative and therapeutic measures.

1. Introduction

Prion diseases or transmissible spongiform encephalopathies (TSEs) are fatal neurodegenerative illnesses afflicting humans and animals. Interest in prion diseases has grown with the possibility that bovine prions may have been transmitted to humans [1, 2].

Considerable experimental data argue that prions are composed largely, if not exclusively, of an abnormal pathogenic isoform of a host-encoded cellular prion protein (PrP^{C}), a glycolipid-anchored glycoprotein that is widely expressed in neurons and glia in the central nervous system [3, 4]. The pathogenic isoform (PrP^{Sc}) results when PrP^{C} undergoes a conformational change, resulting in a post-translational modification in which its normal, α-helical structure is changed into the toxic β-sheet conformation. Subsequently, PrP^{Sc} would be able to induce the transconformation of its host isomer PrP^{C} into PrP^{Sc} [5]. PrP^{Sc} is isolated from tissue as a highly aggregated and detergent insoluble polymer which has markedly increased resistance to proteolysis.

Currently there is no effective therapy for prion diseases. A better understanding of the molecular mechanisms and energetic basis underlying the structural conversion of PrP^{C} into the infectious protein topology is needed for a therapeutic approach. Although the purified recombinant PrP^{C} can be converted *in vitro* (under defined reaction conditions) into a conformation having features in common with the infectious isoform [6], the infectivity of such a misfolded conformation has not been proven so far. The reason for this setback may be that

(i) the experimental conditions used do not lead to the alternative folded form associated with infectivity, and/or

(ii) the process of conversion may require the binding of PrP^{C} to a still unidentified molecule.

Without excluding the role of a cofactor, the current work is placed within the framework of the first option, which supposes that the acquisition of the pathologic structure depends on folding pathways, which are not easily attained. We have used high hydrostatic pressure conditions, *in vitro*, to identify new prion protein topologies. Because pressure is likely to induce a polypeptide chain to undergo a different conformational change with respect to other denaturing agents [7], this much less used thermodynamic parameter provides an elegant alternative to investigate new aspects of protein misfolding and refolding to alternative conformations, and may thus help to unravel the structural ambiguity of prion proteins.

Here, we provide insights into the pressure-induced folding–unfolding and aggregation processes of the prion protein, and we characterize a PrP^{Sc}-like conformer or structural intermediate on the pathway leading to PrP^{Sc}.

2. Experimental procedures

Prion protein. Recombinant $SHaPrP_{90-231}$ was prepared from *E. coli* as described in [8]. Proteins were stored at $-20\,^{\circ}C$ in ultrapure water containing 0.005% sodium azide. Protein concentration was determined spectrophotometrically using a molar extinction coefficient at 278 nm of 25 327 $M^{-1}\ cm^{-1}$.

2.1. Structural characterization under pressure or high temperature

For high-pressure experiments, the protein was dissolved in 20 mM Tris–HCl buffer. This buffer was selected for its relatively small pressure pH dependency [9]. Following each pressure change, typically in steps of 30 MPa, the sample was allowed to equilibrate for 5 min before the next measurement. Spectral measurements (absorbance and fluorescence) were performed using a thermostated high pressure cell [10] which was placed into the sample compartment of the spectrometers.

For experiments as a function of temperature, the protein was dissolved in 20 mM sodium phosphate buffer. The temperature was increased in steps of 3 °C. The sample was allowed to equilibrate at the corresponding temperature for 5 min prior to making measurements.

2.1.1. Absorbance spectroscopy. The UV spectra were recorded with a Cary 3E (Varian) spectrophotometer, between 260 and 305 nm, in steps of 0.1 nm (1 nm bandpath). The fourth derivatives of the UV spectra were evaluated as described [11, 12]. The resulting derivative spectra reflect the averaged polarities of the tyrosines and tryptophans side chains.

2.1.2. Fluorescence spectroscopy. Fluorescence emission spectra were recorded on an Aminco-Bowmann Series 2 luminescence spectrometer (SLM Aminco). ANS (8-anilino-1-naphthalene sulfonate) and ThT (thioflavin-T) were used as extrinsic fluorescence probes. For ANS binding studies, fluorescence was excited (4 nm slit) at 360 nm, and emission spectra (8 nm slit) were collected (accumulation of three scans) between 400 and 600 nm. The final ANS concentration was 50 μM. For ThT, assays were performed with a final ThT concentration of 10 μM. Fluorescence emission spectra (average of three scans) were obtained with an excitation wavelength of 442 nm and excitation and emission slits of 4 and 8 nm, respectively. Protein aggregation was followed by monitoring the changes in light scattering intensity at 340 nm (4 nm slit widths).

2.2. Structural characterization at atmospheric pressure

2.2.1. ThT and ANS binding. Aliquots of soluble and aggregated PrP (2 mg ml^{-1}) were diluted 40 times with 50 mM Tris–HCl, pH 8.5, and incubated with either 10 μM ThT for 1 min or 50 μM ANS for 10 min at room temperature before monitoring fluorescence. Fluorescence measurements were performed at 21 °C on a FluoroMax-2 fluorimeter (Jobin Yvon-Spex) with a 1 cm rectangular cuvette. For ANS spectra, excitation was at 385 nm (2 nm slit). Each emission spectrum (from 400 to 600 nm) (2 nm slit) was the average of four scans. The ThT emission spectra were recorded after excitation at 450 nm (excitation and emission slits were 4 nm), with each spectrum being the average of four scans.

2.2.2. Circular dichroism (CD) spectroscopy. CD spectra were recorded at ambient conditions using a J810 spectropolarimeter (Jasco). A 0.1 cm optical path length quartz cell was used to record spectra of proteins in the far UV region (190–260 nm). Baseline corrected CD spectra were acquired at a scan speed of 20 nm min^{-1}, a 1 nm bandwidth, and a response time of 1 s. The sample compartment was purged with pure dry nitrogen. Spectra were signal-averaged over four scans.

2.2.3. FTIR spectroscopy. FTIR spectra were recorded at ambient conditions on an IFS28 spectrometer equipped with a DTGS detector (Bruker). The spectra (accumulation of 100 scans) were recorded at a spectral resolution of 2 cm^{-1}. For a comparison of soluble and aggregated protein, all spectra were recorded with dry samples. Samples were prepared by protein deposition onto a fluorine plate, where the solvent was allowed to evaporate overnight at room temperature.

2.2.4. Congo red staining and birefringence. Aggregated protein suspension was air-dried on a glass microscope slide. The protein film was immersed in a solution containing 2% (w/v) Congo red and 80% (v/v) ethanol/water for 15 min and then rinsed by immersion in

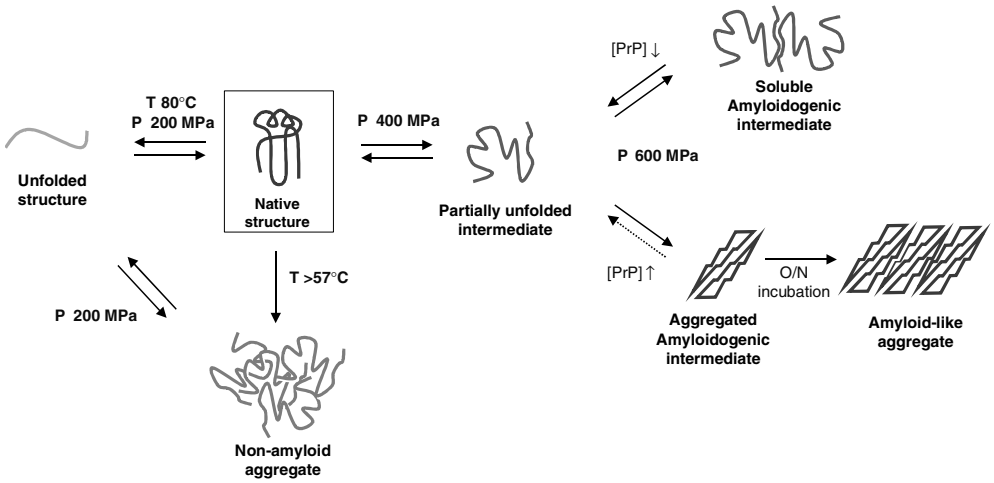

Figure 1. A schematic representation of the temperature- and pressure-induced misfolding process of PrP leading to the formation alternative prion protein topologies.

90% ethanol for 2 min and dried. Birefringence was observed with a Leica DM IRM light microscope (Leica Microsystems) equipped with a polarizer.

2.2.5. Proteinase K resistance. The protease resistance was assayed by incubating sample aliquots (soluble or aggregated PrP) in 20 mM Tris–HCl pH 8.5 containing various concentrations of proteinase K (PK) for 1 h at 37 °C. Protein–PK ratios were from 166:1 to 3:1. The digestion reaction was terminated by addition of Pefabloc (Roche Diagnostics GmbH) to a final concentration of 3 mM. Finally, the sample was assessed by SDS-PAGE.

3. Results and discussion

We have developed a method for the effective cloning, overexpression in *E. coli* and purification to homogeneity of Syrian golden hamster prion protein ($SHaPrP_{90-231}$) [8]. The recombinant protein was identified by monoclonal antibodies and its integrity was confirmed by electrospray mass spectrometry (ES/MS). Correct folding was assessed by circular dichroism (CD) spectroscopy. The purified protein had the structural characteristics of PrP^C.

In this paper we describe the use of high pressure as a thermodynamic parameter, capable of creating *in vitro* conditions under which recombinant prion proteins can be refolded into different conformations. Such *in vitro* isoforms of prion protein, obtained in the current work, are shown schematically in figure 1. Our findings are potentially interesting as they unravel folding and aggregation pathways of a mammalian prion protein, which are not observed by conventional methods (i.e. heat and/or chemical induced unfolding). The results obtained fit well with the wide variety of folding–unfolding scenarios emerging from the so-called 'new view' of protein folding (illustrated by the concept of the folding funnel) [13]. Interestingly, our studies of hamster prion protein [14] have shown that certain steps of its structural changes and aggregation could be made reversible or irreversible by modulating temperature and pressure.

At high temperature (pH 7.0), recombinant hamster prion protein undergoes aggregation and changes from a predominantly α-helical to β-sheet conformation. This process was reflected by a sharp increase in light scattering intensity, and a strong enhancement of the

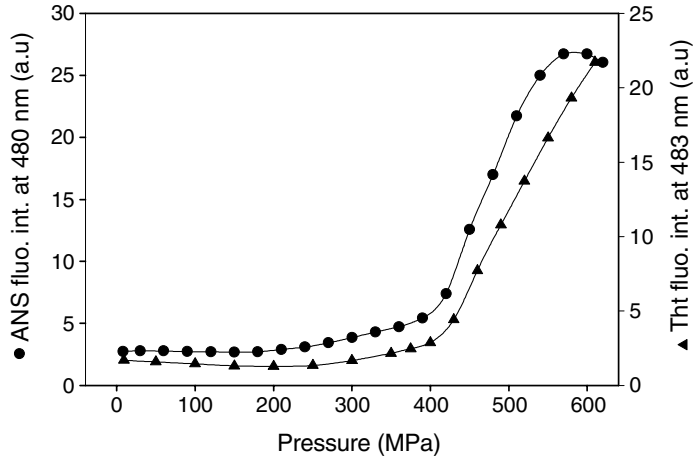

Figure 2. *In situ* ThT and ANS binding upon increasing pressure monitored by the change in fluorescence intensity at the emission maximum wavelength, 480 and 483 nm, respectively. It is worth indicating that the enhanced fluorescence intensity observed arises from the particular spectral properties of both extrinsic probes upon binding to protein and not to scattered light.

1620 cm^{-1} component of its FTIR spectrum. We then applied high pressure (200 MPa) to the temperature-induced aggregate. As revealed by different spectroscopic techniques (light scattering, UV absorbance, FTIR and CD analysis), the aggregation was reversed, and the original tertiary and secondary structures were recovered at ambient pressure, after pressure release. In addition, analysis at high temperature, in the absence of protein aggregation, was possible by maintaining a constant pressure of 200 MPa. The application of hydrostatic pressure thus allowed us to study reversibly the heat-induced equilibrium unfolding.

Prion protein unfolding as a function of high pressure was also investigated. Simple two-state, reversible unfolding transitions were observed at pH 7.0, as monitored by spectral changes in the UV absorbance. ANS binding to nonnative patches of exposed hydrophobic residues suggested that complete unfolding of PrP was not achieved at high pressure. From UV absorbance experiments, it was apparent that in the unfolded state (for both pressure and temperature experiments), on average, the tyrosine residues are more exposed to the aqueous solvent, and the formerly two well-exposed tryptophan display interactions with nonpolar residues. Although there was no evidence of the appearance of scattering aggregates at high pressure, reversible ThT binding was observed over 400 MPa. This suggests that, at pressures above 400 MPa, a structural change from a partially unfolded intermediate to a metastable oligomeric structure took place. Heat- and pressure-induced conformers differed in their unfolding free energy and in their ANS and ThT binding capacities. Binding was observed only under high pressure. This suggests that heat and pressure do not lead to identical unfolded structures, an observation that has been made also for other proteins [15, 16]. Therefore, pressure appears as an interesting tool to explore new conformational coordinates of the prion protein conformational landscape.

To investigate further the origin of the enhanced ThT binding at high pressure, we performed unfolding at a higher protein concentration (2 mg ml^{-1}). After treatment of PrP, at pH 8.5 and 40 °C, to pressures above 400 MPa, the above mentioned ThT-binding intermediate underwent aggregation. After pressure release, the turbidity of the solution was observable with the naked eye. Two extrinsic fluorescence probes, ANS and ThT, were used to emphasize *in situ*

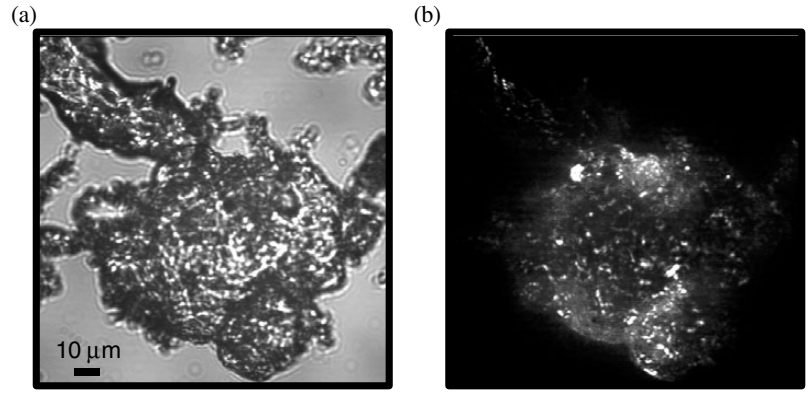

Figure 3. Congo red birefringence in pressure-induced PrP aggregates formed at pH 8.5 and 40 °C upon overnight treatment at 600 MPa, followed by sonication after pressure release. Aggregates were stained with Congo red and observed under bright field (a) or by polarization microscopy (b).

different aspects in the pressure-induced aggregation process. As shown in figure 2, applying high pressure (>400 MPa) to a sample of protein containing ANS or ThT led to a gradual and large increase in the fluorescence intensity of the corresponding probe, indicating a partially unfolded and amyloidogenic nature of the intermediates participating in aggregation. Further characterization of the PrP aggregates obtained after immediate decompression revealed that aggregation was accompanied by an increase in β-sheet content and an acquired resistance to proteolysis (resistance to proteinase K). After overnight incubation of PrP at 600 MPa and 40 °C, assembly processes between aggregates into higher order and packed aggregates, evidenced by protein deposition, led to the formation of amyloid-like structures which showed green birefringence when viewed under polarized light after Congo red staining (figure 3). Amyloid-like formation was also monitored by ThT and ANS fluorescence. Binding at atmospheric pressure to the mature aggregated species resulted in a clear increase in both ThT and ANS fluorescence signal, indicating amyloid-like structural features.

Although the pressure-induced aggregates obtained in this work have features in common with the infectious form, it is still unclear whether they are capable of causing neuronal degeneration and disease. To check this possibility, infectivity bioassays of pressure-induced PrP aggregates are in progress. The characterization of a PrP^{Sc}-like conformer or intermediate on the pathway to PrP^{Sc} would certainly open new avenues for structure-based drug design studies pointed to interfere with aggregation or to prevent amyloid-related toxicity. Much remains to be learned about the so-called 'conformational diseases', of which TSEs and Alzheimer's disease are striking examples, but it is clear that insights into the conformational changes of the involved proteins, like those described above, may pave the way for further revealing the potential of high pressure studies to amyloid diseases.

Acknowledgments

JT acknowledges an INSERM Poste-Vert fellowship. This work is supported by GIS—prions (Ministery of Research), ATC—prions (INSERM) and Human Science Frontier Program (HSFP).

References

[1] Chazot G, Broussolle E, Lapras C, Blattler T, Aguzzi A and Kopp N 1996 *Lancet* **347** 1181
[2] Bateman D, Hilton D, Love S, Zeidler M, Beck J and Collinge J 1995 *Lancet* **346** 1155–6
[3] Oesch B *et al* 1985 *Cell* **40** 735–46
[4] Stahl N, Borchelt D R, Hsiao K and Prusiner S B 1987 *Cell* **51** 229–40
[5] Prusiner S B, Scott M R, DeArmond S J and Cohen F E 1998 *Cell* **93** 337–48
[6] Glockshuber R 2001 *Adv. Protein Chem.* **57** 83–105
[7] Balny C, Masson P and Heremans K 2002 *Biochim. Biophys. Acta* **1595** 3–10
[8] Alvarez-Martinez M T, Torrent J, Lange R, Verdier J M, Balny C and Liautard J P 2003 *Biochim. Biophys. Acta* **1645** 228–40
[9] Kitamura Y and Itoh T 1987 *J. Sol. Chem.* **16** 715–25
[10] Lange R, Frank J, Saldana J L and Balny C 1996 *Eur. Biophys. J.* **24** 277–83
[11] Lange R and Balny C 2002 *Biochim. Biophys. Acta* **1595** 80–93
[12] Torrent J, Connelly J P, Coll M G, Ribo M, Lange R and Vilanova M 1999 *Biochemistry* **38** 15952–61
[13] Dill K A and Chan H S 1997 *Nat. Struct. Biol.* **4** 10–9
[14] Torrent J, Alvarez-Martinez M T, Heitz F, Liautard J P, Balny C and Lange R 2003 *Biochemistry* **42** 1318–25
[15] Takeda N, Kato M and Taniguchi Y 1995 *Biochemistry* **34** 5980–597
[16] Zhang J, Peng X, Jonas A and Jonas J 1995 *Biochemistry* **34** 8631–41